Polym. Bull. (2010) 64:291–302
DOI 10.1007/s00289-009-0187-z

ORIGINAL PAPER

Dynamic rheology–morphology relationship of PP/EPDM blends prepared by melt mixing under Sc-CO_2

Yang Zhao · Han-Xiong Huang · Yu-Kun Chen

Received: 12 November 2008 / Revised: 16 April 2009 / Accepted: 4 October 2009 /
Published online: 15 October 2009

Abstract It was demonstrated that the high mixing efficiency of twin screw extruder (TSE) helped to disperse the ethylene–propylene–diene terpolymer (EPDM) domains in polypropylene (PP) matrix, but could not lead to the uniform distribution of EPDM phase with small sizes because of the thermodynamical immiscibility between PP and EPDM. So supercritical carbon dioxide (Sc-CO_2) was environmentally and economically introduced to the twin screw extrusion to assist the melt mixing of PP and EPDM. The scanning electron microscopy photographs showed that co-continuous phase morphology was formed to some extent for the PP/EPDM 60/40 blend prepared with Sc-CO_2, especially with 2.5 wt% Sc-CO_2. This was the one important reason for that the complex viscosity and storage modulus of PP/EPDM 60/40 blend increased with the increase of Sc-CO_2 concentration.

Keywords Polymer blend · Supercritical carbon dioxide · Dynamic rheology · Melt mixing

Introduction

Polypropylene (PP) as a thermoplastic resin has a number of advantages, such as low cost, good processability, and good physical properties. However, its application as an engineering thermoplastics is somewhat limited because of its relative poor impact resistance. Many studies have been carried out on the blending of PP with elastomers to improve its impact toughness, and ethylene–propylene–diene terpolymer (EPDM) is one of the elastomers extensively used as the

Y. Zhao · H.-X. Huang (✉) · Y.-K. Chen
Laboratory for Micro Molding and Polymer Rheology, Center for Polymer Processing Equipment and Intellectualization, South China University of Technology, Guangzhou, People's Republic of China
e-mail: mmhuang@scut.edu.cn

component of the blends [1–4]. Though PP and EPDM have similarity in chemical structure, they are not compatible [5, 6], which generally leads to poor interface adhesion and non-uniform dispersed phase in the blend with undesirable mechanical properties, that is to say, the EPDM does not effectively toughen the PP.

Twin screw extruder (TSE), which is commonly used in polymer blending, has high mixing efficiency. However, the control of the morphology of the dispersed phase in polymer blends depends more on the interfacial interaction than the viscosity ratio, processing conditions, etc. [7]. Therefore, during blending PP matrix with immiscible EPDM, using the TSE with high mixing ability, the uniform distribution of EPDM domains with small sizes is difficult to be obtained without introducing other methods. These methods include the addition of various compatibilizers [3, 6–8], the application of ultrasound irradiation [9–11] etc. The addition of compatibilizers improves the interface adhesion of immiscible polymers. Feng and Isayev [9] and Chen and Li [10, 11] revealed that when applying ultrasound vibration to PP/EPDM blend melt at the die, smaller and more homogenous dispersed EPDM domains, as well as good adhesion between EPDM and PP matrix were formed. The addition of fillers [12–16] is another way to further toughen the PP/EPDM blends, because the fillers are used to generate special distribution structures in the blends, which improves the mechanical properties.

Lee et al. [17] and Elkovitch et al. [18] found that supercritical carbon dioxide (Sc-CO_2) injection during prolonged batch mixing (at a residence time of tens of minutes) or extrusion (at a residence time of seconds) leads to smaller size of dispersed phase with more uniform distribution in blends. Sc-CO_2 has characteristics such as gas-like diffusivity and viscosity and liquid-like density. In particular, it has been used in a wide range of applications due to environmental-friendly merit and lower critical point (critical temperature: 31.8 °C, critical pressure: 7.38 MPa). The Sc-CO_2 injected into the molten polymer acts as a lubricant, which reduces the chain–chain interactions, swells the polymer, and increases the polymer free volume. Therefore, important functions of Sc-CO_2 are the plasticization of the polymer and the change of its physical properties, including the reduction of glass transition temperature, interfacial tension, and melt viscosity [19, 20].

In this study, an industrial-scale TSE was used for the continuous extrusion of PP/EPDM blends with the Sc-CO_2 injected into the barrel. The aim was to investigate not only the effects of Sc-CO_2 on the rheological behavior and morphology of the PP/EPDM blends, but also the relationship between them.

Experimental

Materials

The PP used was grade J501 manufactured by Sinopec Group Guangzhou, China. Its melt flow index was 2.7 g/10 min, which was measured on a melt indexer (T.O. MP993A, America) at 230 °C and under the load of 2.16 kg. The EPDM (4045,

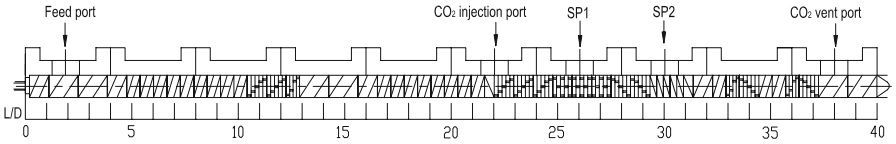

Fig. 1 Schematic of extruder screw configuration used in this study

54 wt% ethylene, $ML_{(1+4)}$ at 100 °C: 45) used was manufactured by Mitsui Petrochemical Industries, Japan.

Experimental equipment and sample preparation

The equipment mainly included a co-rotating TSE (35 mm diameter, 40 length-to-diameter ratio) and a CO_2 injection system. The CO_2 injection system had a cylinder, a positive displacement syringe pump (500D, ISCO), and back pressure regulators. The connection of units was described in a previous article [21], and the screw configuration used in this study is shown in Fig. 1. Along the extruder, there were two online sample collecting positions denoted as SP1 and SP2 in Fig. 1.

A mixture containing PP and EPDM in ratio of 80:20 or 60:40 by weight was fed to the TSE. The compounding was carried out at a feed rate of 3 kg/h, a screw speed of 100 rpm, and the temperature profiles of 140–140–140–140–140–140–140–170–170–170 °C from the hopper to the pelletizing die. The Sc-CO_2 was injected to the cylinder at the position of about 22 times of screw diameter (D) away from the hopper. The CO_2 in the syringe pump was compressed to 20 MPa, and the flow rate of CO_2 was set to keep the CO_2 concentration to be 0, 1, and 2.5 wt% of the feed rate of the PP/EPDM mixture. At the position of about 38D from the hopper, CO_2 was vented by vacuum pump. The extruded blend strands were pelletized after direct solidification in water bath. Disks with a size of $\phi 25 \times 1$ mm were immediately compressed from the blend melt just out of the die exit.

Characterization

Rheological measurement

The melt shear viscosities of pure PP and EPDM were measured using the Haake ProFlow online rheometer, which was side-mounted at the exit of a single screw extruder with a screw diameter of 25 mm and a length–diameter ratio of 25:1. The ProFlow system continuously diverted a small flow of material from the end of extruder and pushed that material through a capillary by means of a melt pump. The pressure before the melt pump was controlled by an automatic bypass valve to avoid the disturbance of the process during the measurement.

Bohlin Gemini 200 Rheometer equipped with a parallel-plate fixture (25-mm diameter) was used in an oscillatory mode to conduct dynamic frequency sweep measurement on the previously prepared disks. Dynamic complex viscosity (η^*) and storage modulus (G') as function of angular frequency (ω) ranging from 0.01 to 100 rad/s were measured by frequency sweep at 150, 170, and 200 °C, respectively.

Before conducting the frequency sweep, amplitude sweep was performed at a controlled stress mode from 1 to 5,000 Pa at a frequency of 1 s^{-1} to determine a fixed strain of 5%, which was used to ensure that the frequency sweep was carried out within the linear viscoelastic range of the PP/EPDM blend investigated. The sample was loaded between two parallel plates with a gap of 1 mm and soaked for 15 min at the test temperature.

Morphology observation

A Hitachi S-520 scanning electron microscope (SEM) was used to observe the phase morphology of extruded PP/EPDM blend strands. The strands were immersed in liquid nitrogen for about 5 min and fractured perpendicular or parallel to the flow direction. Then, cryogenically fractured specimens were etched by cyclohexane at room temperature for 24 h to remove the EPDM phase. Before the SEM observation, the etched surfaces were coated with gold.

In order to quantitatively assess the SEM micrographs in respect of the morphology of EPDM domains, the SEM gray-level image was converted into a binary image using Scion image software (Scion Corp.), specifying a brightness threshold setting. On analyzing the SEM photomicrographs of samples, the mean particle diameter $\bar{d}$ was calculated by the following equation:

$$\bar{d} = \frac{\sum_{i=1}^{N} d_i}{N} \tag{1}$$

where d_i is the single particle diameter, N is the number of particles shown in the SEM micrograph.

Results and discussion

Rheological properties

In two-phase polymer blending, the viscosity ratio of the dispersed phase to the matrix plays an important role in controlling the domain size of the dispersed phase, which exhibits a minimum value when the viscosity ratio is close to one, and increases as the viscosity ratio increases [22]. Figure 2 shows the apparent melt shear viscosity as a function of shear rate for pure PP and EPDM at 200 °C. The shear viscosity of EPDM is obviously higher than that of PP, and the viscosity ratio of the EPDM to PP in the shear rates of (1–7) × 10^2 s^{-1} is 2.3–2.5.

The dynamic rheological measurement is an indirect method to probe the morphologies of polymer blends and provides fundamental insights about their viscoelastic properties. Figure 3 shows the complex viscosity η^* and storage modulus G' as a function of frequency at 150, 170, and 200 °C for PP/EPDM blends prepared with different Sc-CO_2 concentration. Figure 4a shows the comparison of η^* and G' between pure PP and EPDM; Fig. 4b shows the comparison of η^* and G' between 20 and 40 wt% EPDM blends prepared without Sc-CO_2. The following observations are worth noting in Figs. 3 and 4.

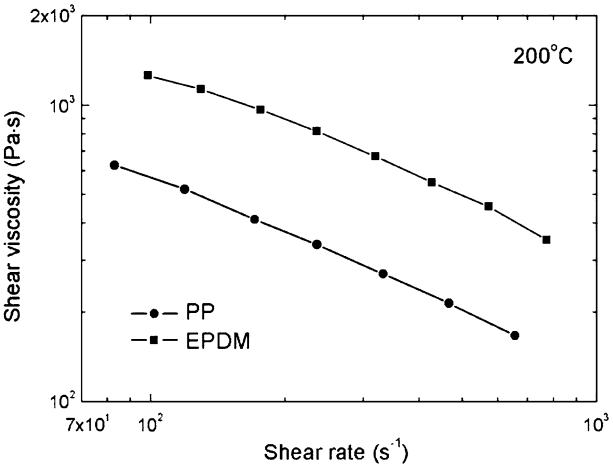

Fig. 2 Shear viscosity of pure PP and EPDM

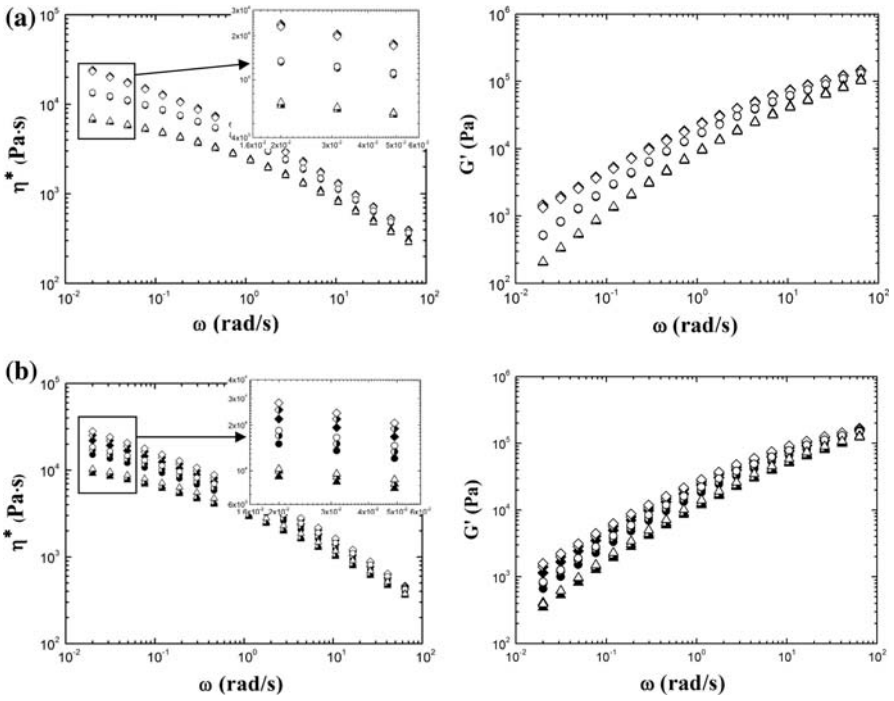

Fig. 3 Complex viscosity η^* and storage modulus G' as a function of frequency ω at 150 (*square symbols*), 170 (*circle symbols*), and 200 °C (*triangle symbols*) for (**a**) 80/20 and (**b**) 60/40 PP/EPDM blends prepared with 0 (*solid symbols*), 1 (*half open symbols*) and 2.5 wt% (*open symbols*) Sc-CO_2

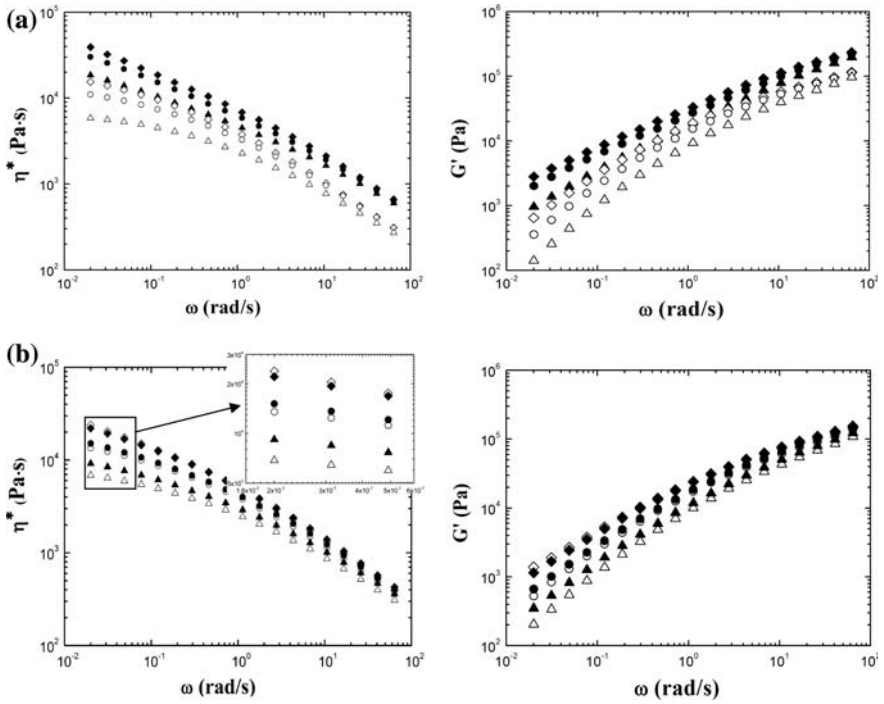

Fig. 4 Complex viscosity η^* and storage modulus G' as a function of frequency ω at 150 (*square symbols*), 170 (*circle symbols*), and 200 °C (*triangle symbols*) for (**a**) pure PP (*open symbols*) and EPDM (*solid symbols*) and (**b**) PP/EPDM 80/20 (*open symbols*) and 60/40 (*solid symbols*) blends prepared without Sc-CO_2

(a) As shown in Fig. 3, the Sc-CO_2 has no influence on the η^* and G' of PP/EPDM 80/20 blend, whereas it results in the increase of 15–30% for η^* and G' of PP/EPDM 60/40 blend.

(b) With or without Sc-CO_2, the decrease of η^* or G' for PP/EPDM 60/40 blend is less than that for PP/EPDM 80/20 blend with the temperature increasing from 150 to 200 °C, as shown in Figs. 3 and 4b.

(c) As shown in Fig. 4b, at low frequencies, the η^* and G' of PP/EPDM 80/20 blend are close to or even slightly higher than those of PP/EPDM 60/40 blend at 150 °C.

The above mentioned three phenomena will be interpreted in section "Relationship between rheology and phase morphology".

Phase morphologies

First, the PP/EPDM blend samples were collected at three different positions online along the TSE without injection of Sc-CO_2 and their brittle fracture surfaces were observed by SEM. Some results are shown in Fig. 5, which displays the phase

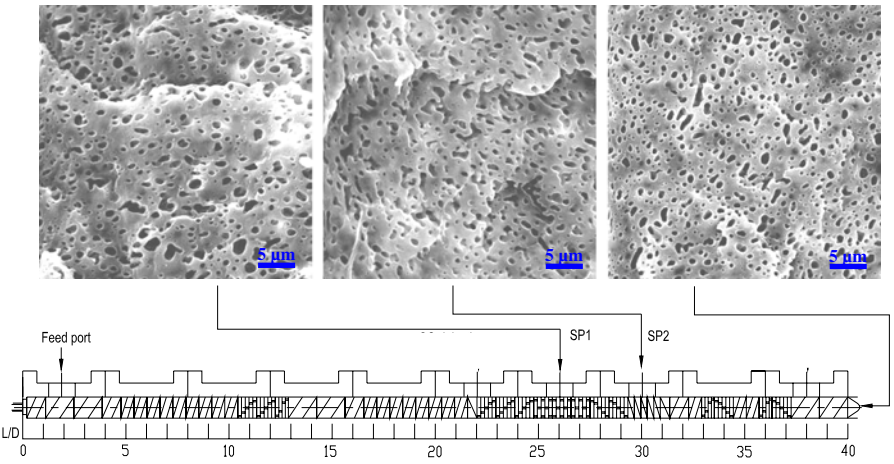

Fig. 5 SEM micrographs on fracture surfaces of PP/EPDM 60/40 blend samples collected from SP1, SP2, and the end of extruder

morphologies of fracture surfaces perpendicular to the flow direction for the PP/EPDM 60/40 blends. The EPDM droplet diameter and their standard deviation for the samples are shown in Table 1. As shown in Fig. 1, a long high shear zone, which consists of kneading elements, is arranged along the screw section from 22*D* to 31*D*. Positions SP1 and SP2 are nearly at the middle and at the end of this high shear zone. As shown in Fig. 5, spherical or ellipsoidal EPDM droplets with some large domains (maximum diameter: 2.33 μm, mean diameter: 0.55 μm, as shown in Table 1) dispersed in the PP matrix are observed in the PP/EPDM blend collected at position SP1. At position SP2, the EPDM phases are deformed to some extent due to the further applied high shear. Downstream, two short high-shear zones are arranged. So, some smaller EPDM droplets can be observed in the blend collected at the end of the extruder, where the maximum and mean diameters of droplets decrease to 1.73 and 0.46 μm, respectively, as shown in Table 1. Therefore, the high shear imposed by kneading elements of screws can effectively reduce the size of EPDM domains, most of them have diameter less than 0.5 μm. However, as shown in Fig. 5, the size distribution of EPDM domains for the blend sample collected at the end of extruder is still nonuniform.

Then, the PP/EPDM blend samples prepared with different concentration of Sc-CO_2 were collected at the end of TSE, and their morphologies were observed on the brittle fracture surface. The results illustrated in Fig. 6 are for the PP/EPDM 60/40 blends. The EPDM droplet diameter and their standard deviation for the blends are shown in Table 1. As can be clearly seen, the injection of Sc-CO_2 leads to the size reduction and distribution uniformity improvement of EPDM phases, as shown on the surface perpendicular to the flow direction, and the breakup of long striations into short platelets or even droplets, as shown on the surface parallel to the flow direction. More interestingly, co-continuous phase morphology is formed to some extent for the 60/40 blend prepared with Sc-CO_2, especially with 2.5 wt% Sc-CO_2, as shown on the surface parallel to the flow direction. As shown in Table 1,

Table 1 EPDM droplet diameters and their standard deviation for PP/EPDM blends

	PP/EPDM 60/40 blends					PP/EPDM 80/20 blends		
	SP1	SP2	Extruder exit			Extruder exit		
	Without CO_2	Without CO_2	Without CO_2	With 1 wt% CO_2	With 2.5 wt% CO_2	Without CO_2	With 1 wt% CO_2	With 2.5 wt% CO_2
Min (μm)	0.08	0.05	0.07	0.03	0.03	0.07	0.05	0.03
Max (μm)	2.33	2.40	1.73	1.55	1.41	1.23	0.67	0.84
Mean (μm)	0.55	0.58	0.46	0.43	0.43	0.36	0.26	0.32
SD	0.33	0.35	0.26	0.22	0.21	0.19	0.11	0.14

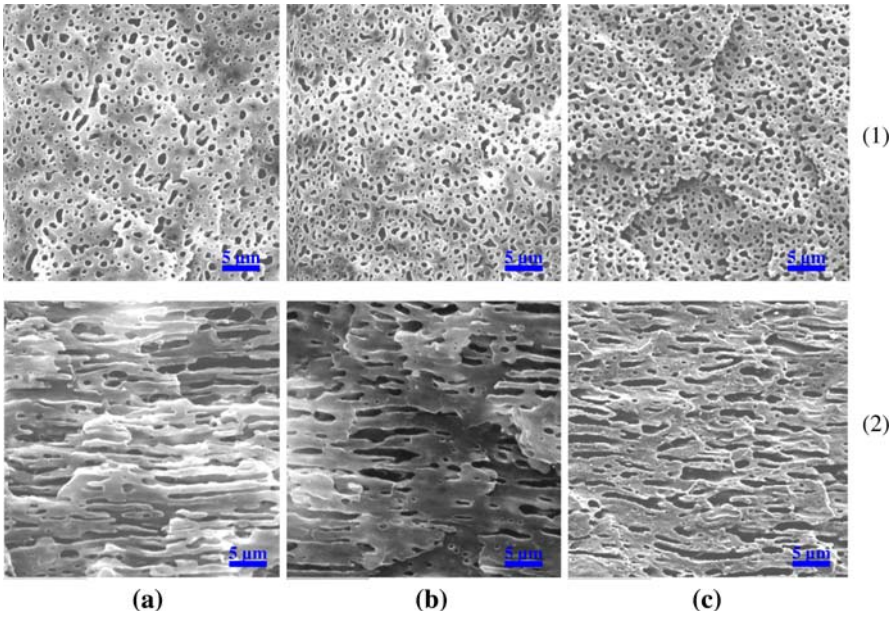

Fig. 6 SEM micrographs on fracture surfaces (1) perpendicular and (2) parallel to the flow direction for PP/EPDM 60/40 blends prepared with (**a**) 0, (**b**) 1, and (**c**) 2.5 wt% Sc-CO_2

the mean diameter of EPDM droplet is decreased and the standard deviation of the droplet diameter is decreased by 15–19% when injecting Sc-CO_2, which quantitatively displays the size reduction and its distribution uniformity improvement of EPDM phases by the addition of Sc-CO_2.

Figure 7 shows the micrographs of brittle fracture surface of PP/EPDM 80/20 blend samples collected at the end of TSE. The EPDM droplet diameter and its standard deviation for the samples are also shown in Table 1. As can be directly observed, the 80/20 blend prepared without Sc-CO_2 exhibits an obviously non-uniform distribution of the EPDM droplets. As can be seen on the surface

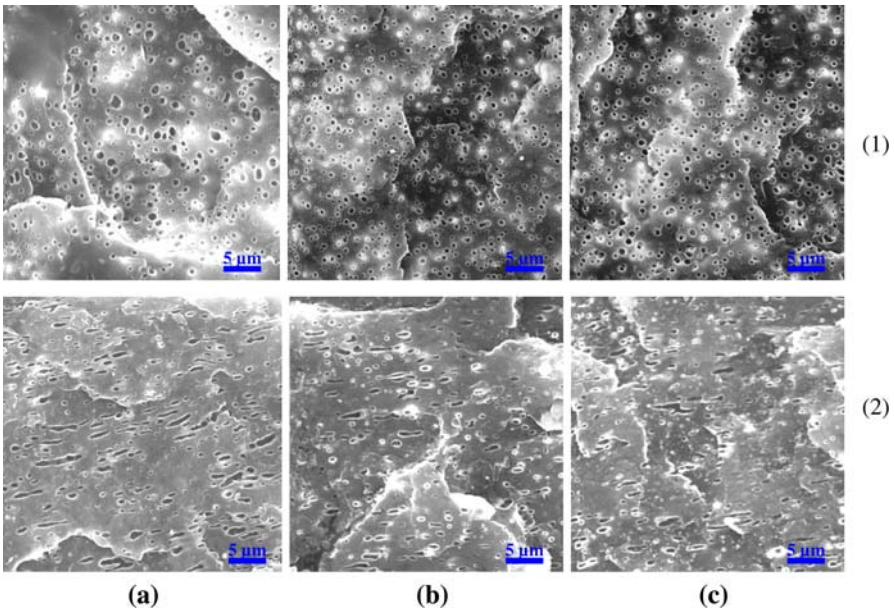

Fig. 7 SEM micrographs on fracture surfaces (1) perpendicular and (2) parallel to the flow direction for PP/EPDM 80/20 blends prepared with (**a**) 0, (**b**) 1 and (**c**) 2.5 wt% Sc-CO_2

perpendicular to the flow direction, some EPDM droplets have large domain size (maximum diameter: 1.23 μm, mean diameter: 0.36 μm); whereas on the surface parallel to the flow direction, some thick EPDM striations with the length about 5 μm are visible. When 1 wt% Sc-CO_2 is injected, the EPDM droplets become smaller (maximum diameter: 0.67 μm, mean diameter: 0.26 μm) and more uniformly distribute in the matrix (the standard deviation of droplet diameter is decreased from 0.19 to 0.11). As can be seen on the surface parallel to the flow direction, some EPDM striations are broken up into shorter striations with about 3-μm length or smaller elliptical droplets. The addition of 2.5 wt% Sc-CO_2 does not further help to promote the dispersion of EPDM domains.

Relationship between rheology and phase morphology

The three phenomena mentioned in section "Rheological Properties" are interpreted as follows. First, as shown in Figs. 6 and 7, the injection of Sc-CO_2 is helpful to promote more uniform distribution of EPDM droplets in the PP matrix for both PP/EPDM 60/40 and 80/20 blends. Compared with the blend samples prepared without Sc-CO_2, this results in higher storage modulus and complex viscosity for the former, whereas has little effect on those for the latter, as shown in Fig. 3. This may be explained as follows. As mentioned above, for the PP/EPDM 60/40 blend, the injection of Sc-CO_2 results in the size reduction and distribution uniformity improvement of EPDM droplets and so shortens the distance between two adjacent dispersed droplets. Moreover, the Sc-CO_2 injection leads to the formation of

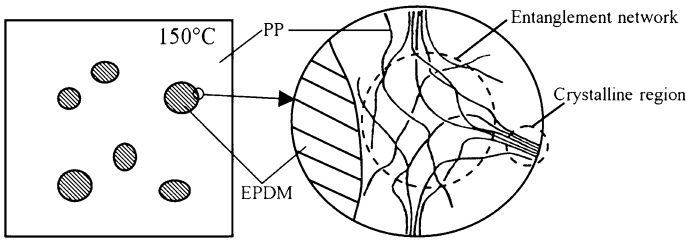

Fig. 8 Schematic representation of microstructures across the interface between PP and EPDM

co-continuous phase morphology to some extent, especially for the blend prepared with 2.5 wt% Sc-CO_2. The droplet–droplet distance reduction and especially the co-continuous morphology formation restrict the mobility of PP and EPDM chains and, thus, increase the complex viscosity and storage modulus of their blend. However, for the PP/EPDM 80/20 blends, the injection of Sc-CO_2 does not reduce the droplet–droplet distance to the extent to result in the collision and coalescence of the EPDM phases and so affect their dynamic rheologies.

Second, as shown in Fig. 4a, the decrease of both complex viscosity and storage modulus of pure PP is more than that of pure EPDM with the temperature increase from 150 to 200 °C. Therefore, the decrease of complex viscosity and storage modulus of PP/EPDM blends with more content of PP is more pronounced with the temperature increase.

Finally, at low frequencies, the storage modulus and complex viscosity of 20 wt% EPDM blend are close to or even slightly higher than those of 40 wt% EPDM blend at 150 °C, as shown in Fig. 4b. The reason for this may be as following. The PP used in this study is a semi-crystalline polymer with the melting temperature (T_m) of about 163 °C. Below T_m, the crystalline regions and non-crystalline regions coexist in PP. According to Qian's results [23], cohesional entanglement networks are formed in the non-crystalline region of polymer. This entanglement networks only can be disentangled at the temperature above T_m. Therefore, at 150 °C, the entanglement networks, together with crystalline regions and EPDM particles, construct a "rigid" network as schematically shown in Fig. 8, which restricts the mobility of polymer chains, and results in the increase of the complex viscosity and storage modulus. These effects are more pronounced in PP/EPDM 80/20 blend due to more content of PP, compared with those in PP/EPDM 60/40 blend.

Conclusions

A Sc-CO_2-assisted polymer extrusion setup was used to prepare the PP/EPDM blends containing 20 and 40 wt% EPDM. The dynamic rheologies and phase morphologies of the PP/EPDM blends were characterized using oscillation-mode rheological test and SEM, respectively. The rheology results demonstrated that for the PP/EPDM 60/40 blend, the complex viscosity and storage modulus increased

with the increase of Sc-CO_2 concentration; whereas the Sc-CO_2 had no influence on the complex viscosity and storage modulus of PP/EPDM 80/20 blend. The complex viscosity and storage modulus more significantly decreased for PP/EPDM 80/20 blend than those for PP/EPDM 60/40 blend with temperature increase from 150 to 200 °C. The SEM micrographs indicated that the Sc-CO_2 was helpful to reduce the domain size and improve distribution uniformity of EPDM phase in PP matrix. Some interesting rheological phenomena were interpreted in respect of the phase morphology.

Acknowledgments The authors acknowledge the financial support provided by the contract grant sponsor—the National Natural Science Foundation of China (contract grant number: 10672061) and Teaching and Research Award Program for Outstanding Young Teachers in Higher Education Institutions of Ministry of Education, People's Republic of China.

References

1. Walker BM (1979) Handbook of thermoplastic elastomers. Van Nostrand Reinhold, New York
2. Whelan A, Lee HS (1979) Developments in rubber technology. Applied Science, London
3. Ao YH, Sun SL, Tan ZY, Zhou C, Zhang HX (2006) Compatibilization of PP/EPDM blends by grafting acrylic acid to polypropylene and epoxidizing the diene in EPDM. J Appl Polym Sci 102:3949–3954
4. Yazdani H, Morshedian J, Khonakdar HA (2006) Effect of maleated polypropylene and impact modifiers on the morphology and mechanical properties of PP/Mica composites. Polym Compos 27:614–620
5. Lopez Manchado MA, Biagiotti J, Kenny JM (2001) Rheological behavior and processability of polypropylene blends with rubber ethylene propylene diene terpolymer. J Appl Polym Sci 81:1–10
6. Kim BC, Hwang SS, Lim KY, Yoon KJ (2000) Toughening of PP/EPDM blend by compatibilization. J Appl Polym Sci 78:1267–1274
7. Shariatpanahi H, Nazokdast H, Dabir B, Sadaghiani K, Hemmati M (2002) Relationship between interfacial tension and dispersed-phase particle size in polymer blends. I. PP/EPDM. J Appl Polym Sci 86:3148–3159
8. Purnima D, Maiti SN, Gupta AK (2006) Interfacial adhesion through maleic anhydride grafting of EPDM in PP/EPDM blend. J Appl Polym Sci 102:5528–5532
9. Feng W, Isayev AI (2004) In situ compatibilization of PP/EPDM blends during ultrasound aided extrusion. Polymer 45:1207–1216
10. Chen Y, Li H (2004) Effect of ultrasound on extrusion of PP/EPDM blends: structure and mechanical properties. Polym Eng Sci 44:1509–1513
11. Chen Y, Li H (2005) Phase morphology evolution and compatibility improvement of PP/EPDM by ultrasound irradiation. Polymer 46:7707–7714
12. Yang H, Zhang XQ, Qu C, Li B, Zhang LJ, Zhang Q, Fu Q (2007) Largely improved toughness of PP/EPDM blends by adding nano-SiO_2 particles. Polymer 48:860–869
13. Arroyoa M, Zitzumbob R, Avalosc F (2000) Composites based on PP/EPDM blends and aramid short fibres. Morphology/behaviour relationship. Polymer 41:6351–6359
14. Wang X, Sun J, Huang R (2006) Influence of the compounding route on the properties of polypropylene/nano-$CaCO_3$/ethylene–propylene–diene terpolymer tercomponent composites. J Appl Polym Sci 99:2268–2272
15. Lopez Manchado MA, Arroyo M, Biagiotti J, Kenny JM (2003) Enhancement of mechanical properties and interfacial adhesion of PP/EPDM/flax fiber composites using maleic anhydride as a compatibilizer. J Appl Polym Sci 90:2170–2178
16. Liang JZ, Li RKY, Tjong SC (2000) Impact fracture behavior of PP/EPDM/glass bead ternary composites. Polym Eng Sci 40:2105–2111
17. Lee M, Tzoganakis C, Park CB (1998) Extrusion of PE/PS blends with supercritical carbon dioxide. Polym Eng Sci 38:1112–1120

18. Elkovitch MD, Lee LJ, Tomasko DL (1999) Supercritical carbon dioxide assisted blending of polystyrene and poly(methyl methacrylate). Polym Eng Sci 39:2075–2084
19. Tomasko DL, Li H, Liu D, Han X, Wingert MJ, Lee LJ, Koelling KW (2003) A review of CO_2 applications in the processing of polymers. Ind Eng Chem Res 42:6431–6456
20. Tomasko DL, Han X, Liu D, Gao W (2003) Supercritical fluid applications in polymer nanocomposites. Curr Opin Solid State Mater Sci 7:407–412
21. Zhao Y, Huang HX (2008) Dynamic rheology and microstructure of polypropylene/clay nanocomposites prepared under Sc-CO_2 by melt compounding. Polym Test 27:129–134
22. Favis BD, Chalifoux JP (1987) Effect of viscosity ratio on the morphology of polypropylene/polycarbonate blends during processing. Polym Eng Sci 27:1591–1600
23. Qian R (2002) Perspectives on the macromolecular condensed state. World Scientific Publishing Co., Singapore